

Stress Analysis of Thin Rimmed Spur Gear with Asymmetric Trochoid

Tufan Gürkan Yılmaz, Oğuz Doğan, Fatih Karpaz

Department of Mechanical Engineering, Uludag University

Uludag University Gorukle Campus, Bursa, Turkey

tufanyilmaz@uludag.edu.tr; doganoguz@uludag.edu; karpaz@uludag.edu

Abstract - Involute spur gears are widely used machine element in many industrial areas. Thin-rimmed spur gears are popular in applications where low weight design and high power transmission are required. The stress occurred on thin-rimmed spur gears are different from standard spur gears due to deformations on rim. For this reason, rim thickness is key parameter for stress analysis of thin-rimmed gears. As rim thickness decreases, the value of maximum bending stress increases and the location of maximum stress is moved bottom of tooth which results in fatigue life reduction. In this study, to decrease maximum bending stress and to move upper the critical point; asymmetric trochoid profile is proposed. Asymmetry is constituted with using rack cutter has different tip radius on sides. This allows using larger tip radius on one side. Firstly, 3D design of spur gear with thin rimmed is realized in CATIA precisely. Then gears are imported to ANSYS package for finite element analysis. Normal force is applied on HPSTC. The rim surface is not fixed to allow rim deformations. The effects of using asymmetric trochoid on value and location maximum bending stress of thin rimmed spur gears is obtained with conducted case studies.

Keywords: Thin rimmed, involute spur gear, asymmetric trochoid

1. Introduction

Involute spur gears with many advantages are the most popular power transmission component in several applications such as automotive and aerospace industries. Today, lightweight concept is a significant objective in design of gears. Thin-rimmed spur gears are used in especially truck gear boxes and helicopter main drive which required low-weight and high load apply. In thin rimmed designs; rim thickness is valid parameter for determining bending stress because of rim deformations. As thin rim is used, the maximum bending stress is increased and the gear is broken on rim not on tooth which is non-desirable result.

Design and stress analysis of solid rimmed spur gears have been investigated for many years [1-4]. Stress analysis of spur gear with thin rimmed is studied for standardization (AGMA, ISO etc.) [5-6]. Oda et al. [7] tried to calculate root stress of spur gear with thin rim by using FEM and experimentally. They pointed that using single tooth model is suitable with adequate precision. They determined that tensile stress reaches its lower value in $1.5 \times m$ rim thickness. According to results of experiment and FEM showed fairly good agreement. Arai et al. [8] studied stress and deformations at tooth and rim in spur gear with thin rim by using FEM and experimental methods. They compared bending strength of spur gear with thin rim and solid spur gear. A practical formula which calculates root stress is offered to estimate bending fatigue limit. It found that FEM results are accordance with experimental ones. Lewicki and Ballarini [9] investigated crack propagation of thin rimmed spur gear for different backup ratios analytically and experimentally. They found that the backup ratio is equal to 0.3, tooth breakage occurred at rim and while backup ratio is equal to 1 and 3.3, tooth breakage is occurred in tooth. For back up ratio is 0.5; the location of breakage is based on initial geometry of crack. Hiremagalur and Ravani [10] calculated root stress of spur gear with thin rim by using complex potential method (CPM) based on elasticity theory and FEM. They validated CPM with FEM and experimental results taken from literature. They determined that when back up ratio is below to 2 and the effect of rim thickness on stress increases. Kramberger et al. [11] studied fatigue life of spur gear with thin rim. They used FEM and BEM methods to evaluate bending stresses. They determined value and location of maximum principle stresses. When used rim thickness as $(2.5-2-1.5) \times m$, the breakage occurred on tooth. For rim thickness is $1 \times m$ the breakage is occurred on rim.

In this study, equations of asymmetric trochoid involute spur gear are generated by MATLAB program based on Litvin's approach. 3D gear design with thin rim is realized in CATIA V5. Finite element analysis is conducted for rim thickness and cutter with symmetric/asymmetric tip radius in ANSYS. According to results; using asymmetric tip radius decreases bending stress of thin rimmed spur gear for each case. On the other side; except one case (Rim thickness is $1.2 \times m$), the location of maximum stress point is move away from tooth bottom.

2. Design of thin rimmed spur gear with asymmetric trochoid

In current study, design of involute spur gear is realized by using Litvin's approach. First, rack cutter's mathematical equations are determined to generate spur gear. Then spur gear tooth equations are derived. $S_n (X_n, Y_n)$ is the coordinate system of rack cutter.

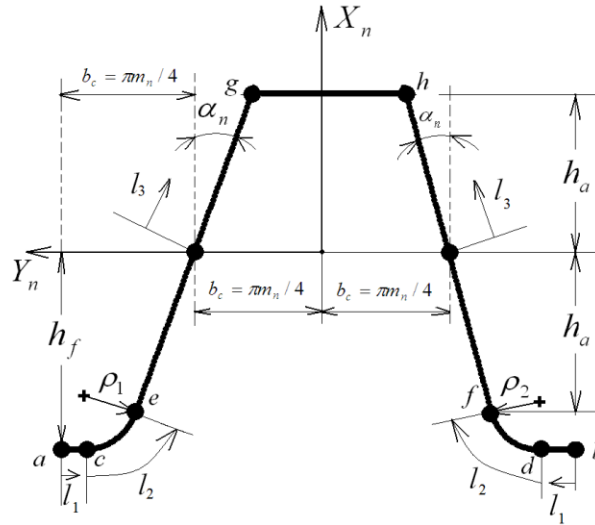


Fig 1: Geometry of asymmetric rack cutter.

The equations of regions in Figure 1 are presented in following equations;

ac-bd region

$$R_n^1 = \begin{bmatrix} -h_f \\ \pm(\frac{\pi m}{2} - l_1) \\ 0 \\ 1 \end{bmatrix} \quad (1)$$

$$0 < l_1 < b_c - h_f \tan \alpha_n + \rho_{1,2} \tan \alpha_n - \rho_{1,2} \sec \alpha_n \quad (2)$$

ce-df region

$$R_n^2 = \begin{bmatrix} -h_f + \rho_{1,2} - \rho_{1,2} \cos l_2 \\ \pm(b_c + h_f \tan \alpha_n - \rho_{1,2} \tan \alpha_n + \rho_{1,2} \sec \alpha_n - \rho_{1,2} \sin(l_2)) \\ 0 \\ 1 \end{bmatrix} \quad (3)$$

$$0 < l_2 < (\frac{\pi}{2} - \alpha_n) \quad (4)$$

eg-fh region

$$R_n^3 = \begin{bmatrix} l_3 \cos \alpha_n \\ \pm(b_c - l_3 \sin \alpha_n) \\ 0 \\ 1 \end{bmatrix} \quad (5)$$

$$\frac{-h_a}{\cos \alpha_n} \leq l_3 \leq \frac{h_a}{\cos \alpha_n} \quad (6)$$

Where, m is the module, z is the teeth number, $\alpha_{n1,2}$ is the pressure angle on sides, h_f is the dedendum factor, h_a is the addendum factor, ρ is the tip radius, $l_{1,2,3}$ is the design parameter of rack cutter, b_c is half of tooth thickness on pitch diameter. + sign indicates the ac-ce-eg region and – sign indicates the bd-df-fh region.

For fully radius rack cutter which is used in this study; ac and bd region are not exist. For this type of cutter; ρ_1 and ρ_2 are defined as following equation;

$$(\rho_1 + \rho_2) = \frac{\frac{\pi m}{2} \cos \alpha_n - 2h_f \sin \alpha_n}{1 - \sin \alpha_n} \quad (7)$$

Unit normal vectors of regions are presented in following equation;

$$n_n^i = \frac{\frac{\partial R_n^i}{\partial l_i} \times k_n}{\left| \frac{\partial R_n^i}{\partial l_i} \times k_n \right|} \quad i=1-3 \quad (8)$$

Where k_n unit normal vector of Z direction.

According to main law of gear meshing, the direction of sliding velocity between rack cutter and spur gear is always perpendicular to unit common normal vector. The expression of this fact is presented in Eq. (8).

$$n_n^i \cdot v_{\text{relative}} = 0 \quad i=1-3 \quad (9)$$

During the manufacturing, the rack cutter moves as $r_{p1} \times \phi_1$ while the generated gear as a workpiece rotates as ϕ_1 . $S_1(X_1, Y_1)$ is the coordinate system of involute spur gear. Relationship between rack cutter and generated gear is shown in Figure 2. In there, x defines as profile shifting.

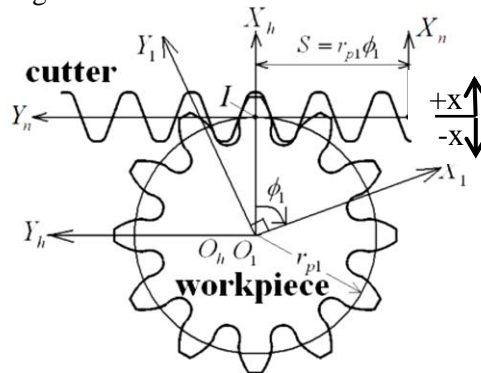


Fig 2: Relation between cutter and generated gear.

Coordinate transformation matrix that transform rack cutter to spur gear and equations of spur gear is presented in the following equations.

$$M_{1n} = \begin{bmatrix} \cos(\phi_1) & -\sin(\phi_1) & 0 & r_{p1}\phi_1 \sin(\phi_1) + r_{p1}\cos(\phi_1) \\ \sin(\phi_1) & \cos(\phi_1) & 0 & -r_{p1}\phi_1 \cos(\phi_1) + r_{p1}\sin(\phi_1) \\ 0 & 0 & 1 & 0 \\ 0 & 0 & 0 & 1 \end{bmatrix} \quad (10)$$

$$R_1^i = M_{1n}^i R_n^i \quad i=1-3 \quad (11)$$

Where M_{1n} is the coordinate transformation matrix and R_1 is matrix of involute spur gear, r_{p1} is pitch diameter.

The coordinates of points of one tooth of involute spur gear are obtained by developed MATLAB program. In Figure 3, the sample result file of program and phases of 3D is illustrated.

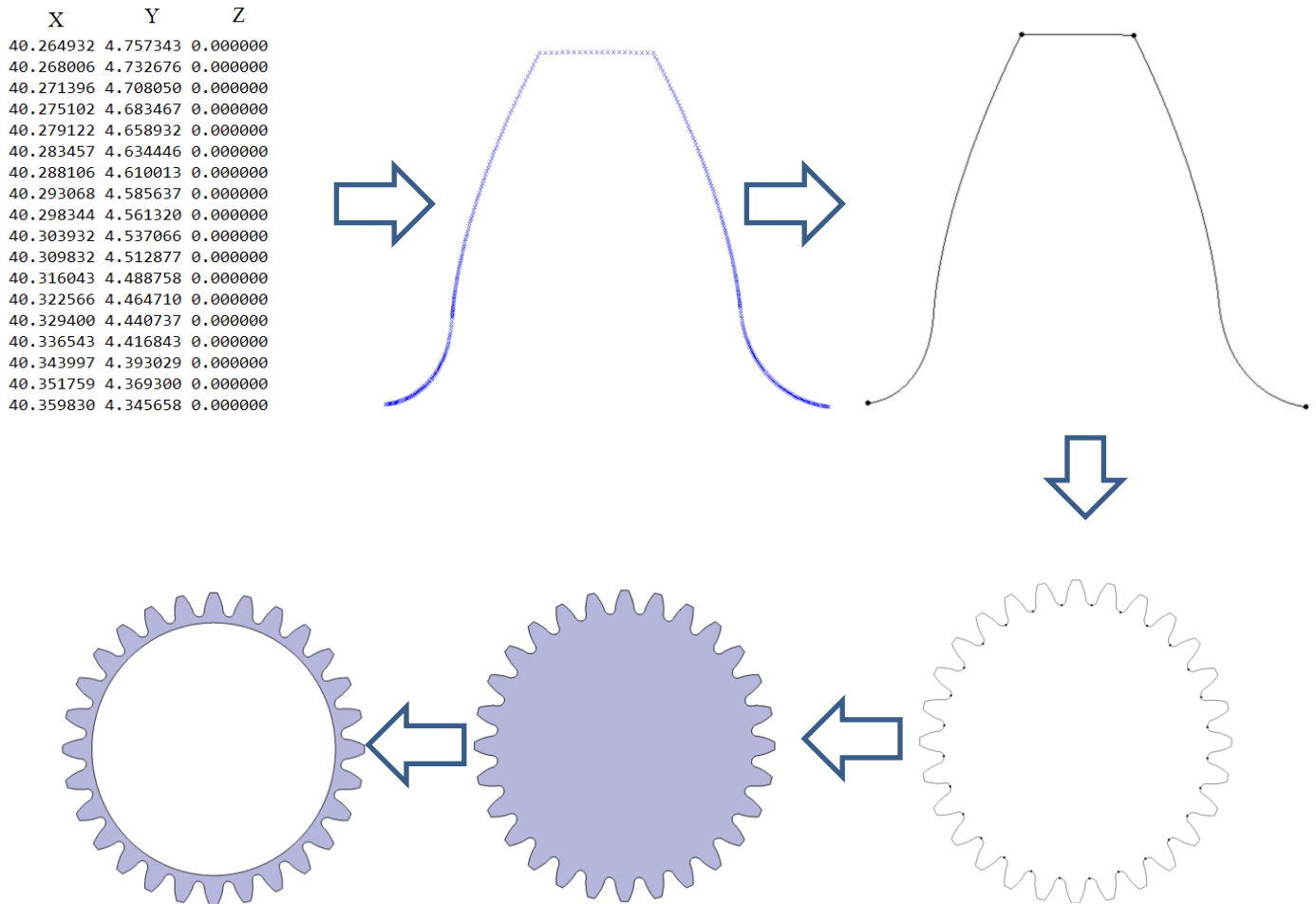


Fig 3: Design phases.

3. Finite Element Analysis and Case Study

In this study, to evaluate effects of asymmetric trochoid spur gear with thin rim; case studies are conducted for different rim thickness and cutter tip radius values. The gear parameters used in analysis are presented in Table 1.

Table 1: Gear properties.

Gear parameters	Case I	Case II
Module- m (mm)	3,18	3,18
Teeth number of pinion- z_1	28	28
Teeth number of gear- z_2	39	39
Pressure angle- α_n ($^\circ$)	20	20
Addendum- h_a ($\times m$)	1	1
Dedendum- h_f ($\times m$)	1.25	1.25
Cutter tip radius- ρ_1 ($\times m$)	0.38	0.58
Cutter tip radius- ρ_2 ($\times m$)	0.38	0.3638
Facewidth- b (mm)	10	10
Rim thickness- S_R ($\times m$)	1.2-1.3-1.4- 1.5	1.2-1.3-1.4- 1.5
Profile shifting- x (mm)	0	0

5 teeth model is used for analysis. Normal force (1000 N) is applied at highest point of single tooth contact (HPSTC). Fixed support is given only on lateral side. Rim region is not fixed to include effects of rim deformations. Boundary condition and mesh is visualized in Figure 4.

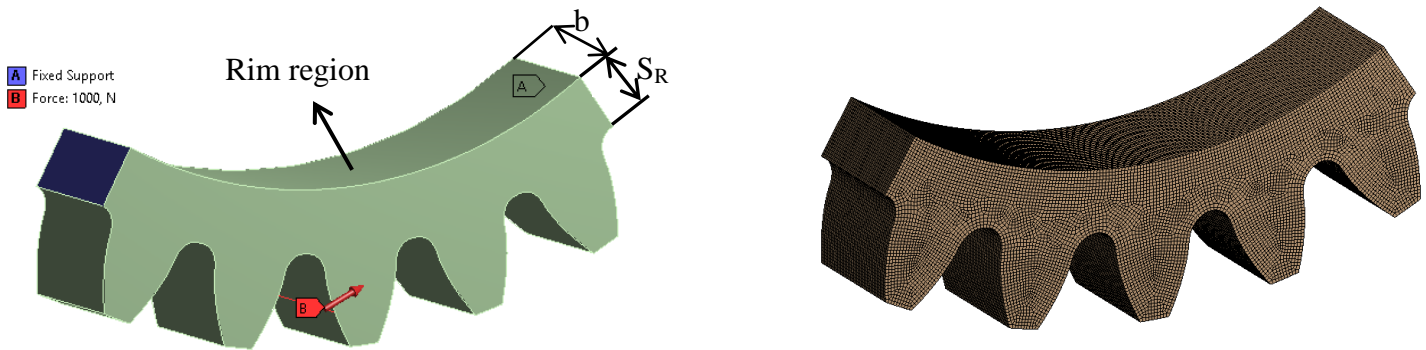


Fig 4: Mesh and boundary condition.

In analysis; hexahedral element type is used with 0.25 mesh size. Model has approximately 229000 element number and has 968514 node numbers.

In Figure 5, the maximum bending stress value is illustrated for each rim thickness (Case I).

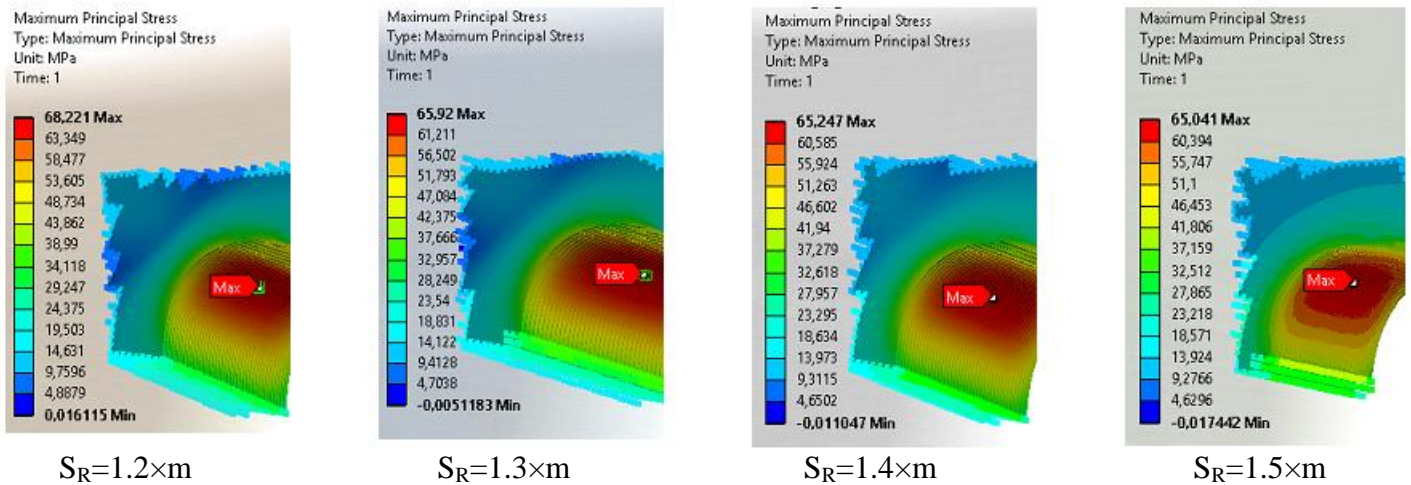


Fig. 5: Bending stress values of Case I.

In Figure 6, the maximum bending stress value is illustrated for each rim thickness (Case II).

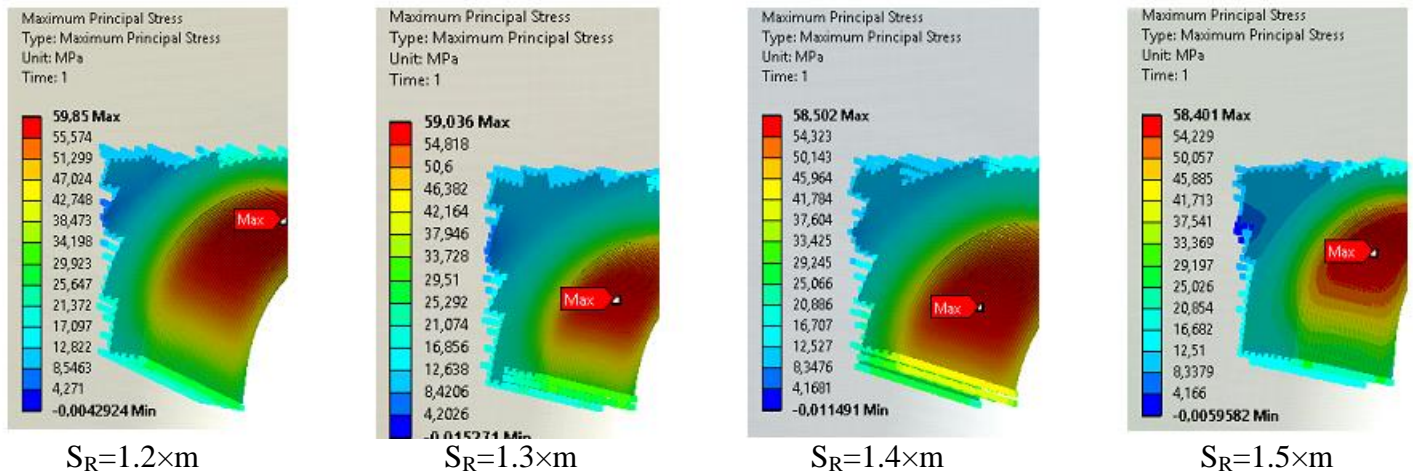


Fig. 6: Bending stress values of Case II.

In Figures, It is clearly stated that using larger tip radius for generating drive side of thin rimmed spur gear decreases maximum bending stress occurred at trochoid region. On the other hand, bending stress decreases with increasing rim thickness slightly.

Decreasing stress values is significant in view of tooth breakage; another significant issue is location of maximum bending stress point. If this location is move to bottom of the tooth, breakage occur in rim region which may result in serious damages. Location of critical point is presented for Case I and II in Table 2.

Table 2: Location of critical point.

CASES	Location of critical point (X_1)	Differences ($X_{1CASE II} - X_{1CASE I}$)
$S_R = 1.2 \times m$ (Case I)	40,576 mm	-0.192
$S_R = 1.2 \times m$ (Case II)	40,384 mm	
$S_R = 1.3 \times m$ (Case I)	40,633 mm	0.32
$S_R = 1.3 \times m$ (Case II)	40,953 mm	
$S_R = 1.4 \times m$ (Case I)	40,737 mm	0.413
$S_R = 1.4 \times m$ (Case II)	41,15 mm	
$S_R = 1.5 \times m$ (Case I)	40,738 mm	0.413
$S_R = 1.5 \times m$ (Case II)	41,151 mm	

4. Conclusion

In this study, the mathematical equation of asymmetric trochoid spur gear with thin rim is presented. The points of tooth are obtained by MATLAB program. Points are imported to CATIA for 3D design with thin rim, and then 3D FEA is conducted for different gear parameter in ANSYS program. The FEA is conducted for different gear parameters which are defined in Table 1. According to results; using asymmetric trochoid in spur gears decreases maximum bending stress. When the cutter tip radius increased from 0.38 to 0.58, the maximum bending stress is decreased nearly %13. Also the location of critical point is move away from tooth bottom for rim thickness is $1.3 \times m$ and above. It is evaluated that effect of rim thickness on bending stress is more significant for rim thickness less than $1.3 \times m$ because of higher rim deformations. Another result indicates that rim thickness $1.4 \times m$ and above effects of asymmetric trochoid in view of location of critical point is eliminated by increasing rim thickness.

References

- [1] F. L. Litvin and A. Fuentes, *Gear Geometry and Applied Theory*. Cambridge, Cambridge University Press, 2004.
- [2] J. R. Colbourne, *the Geometry of Involute Gears*. Newyork, Springer Verlag, 2012.
- [3] E. Buckingham, *Analytical Mechanics of Gears*. Courier Corporation, 1988.
- [4] S. P. Radzevich and W. D. Darle, *Handbook of Practical Gear Design*. CRC press, 1994.
- [5] *Fundamental Rating Factors and Calculation Methods for Involute Spur and Helical Gear Teeth*. ANSI/AGMA 2001-B88, 1999.
- [6] *Calculation of Load Capacity of Spur and Helical Gears*, ISO 6336, 2006.
- [7] S. Oda et al., "Stress analysis of thin rim spur gears by finite element method," *Bulletin of JSME*, vol. 24, no. 193, pp. 1273-1280, 1981.
- [8] N. Arai et al., "Research on bending strength properties of spur gears with a thin rim," *Bulletin of JSME*, vol. 24, no. 195, pp. 1642-1650, 1981.
- [9] D. G. Lewicki and R. Ballarini, "Effect of rim thickness on gear crack propagation path," *Journal of Mechanical Design*, vol. 119, no.1, pp. 89-95, 1997.
- [10] J. Hiremagalur and B. Ravani, "Effect of backup ratio on root stresses in spur gear design," *Mechanics Based Design of Structures and Machines*, vol. 32, no. 4, pp. 423-440, 2004.
- [11] J. Kramberger et al., "Numerical calculation of bending fatigue life of thin-rim spur gears," *Engineering Fracture Mechanics*, vol. 71, no. 4, pp. 647-656, 2004.